

Automated monitoring and analysis of social behavior in *Drosophila*

Heiko Dankert^{1,2}, Liming Wang², Eric D Hoopfer², David J Anderson² & Pietro Perona¹

We introduce a method based on machine vision for automatically measuring aggression and courtship in *Drosophila melanogaster*. The genetic and neural circuit bases of these innate social behaviors are poorly understood. High-throughput behavioral screening in this genetically tractable model organism is a potentially powerful approach, but it is currently very laborious. Our system monitors interacting pairs of flies and computes their location, orientation and wing posture. These features are used for detecting behaviors exhibited during aggression and courtship. Among these, wing threat, lunging and tussling are specific to aggression; circling, wing extension (courtship 'song') and copulation are specific to courtship; locomotion and chasing are common to both. Ethograms may be constructed automatically from these measurements, saving considerable time and effort. This technology should enable large-scale screens for genes and neural circuits controlling courtship and aggression.

How are innate behaviors programmed into the genome? Answering this question requires identifying the genes that control specific behaviors, the neural circuitry on which they act, and how this circuitry controls behavior^{1–5}. This may be attempted in model organisms such as the nematode *Caenorhabditis elegans* and the fruit fly *Drosophila melanogaster*, thanks to the abundant genetic tools for marking, mapping and manipulating specific populations of neurons^{6,7}, thereby enabling large-scale genetic and functional screens^{8,9}.

Social behaviors, such as courtship and aggression, are of particular interest because they have strong innate components. Mating has been studied in both *D. melanogaster* and *C. elegans* using a combination of molecular genetic and cellular approaches^{5,10}. *Drosophila* is unique among invertebrate genetic model organisms in that it exhibits both courtship and aggression^{11–14}.

Measuring animal behavior is difficult. Both aggression and courtship consist of rich ensembles of stereotyped behaviors, which often unfold in a characteristic sequence^{13,15}. Currently these behaviors are measured manually, which is slow and laborious. Subjective decisions by the observer may lead to difficulty in reproducing experiments. Furthermore, human observers may fail

to detect behavioral events that are too quick or too slow and may miss events owing to flagging attention. These constitute substantial obstacles to conducting large-scale behavioral screens.

These limitations could be overcome through automation. The first step toward measuring behavior is tracking (that is, measuring the position and orientation of animals over time). Machine vision systems have been designed for tracking houseflies¹⁶, mice¹⁷, ants¹⁸, bees¹⁹, single *Drosophila* in three dimensions²⁰ and for measuring *Drosophila* locomotion^{9,21,22}, showing promising accuracy and flexibility. However, we do not yet have systems for measuring complex behaviors automatically. A machine vision apparatus that detects lunging, an aggressive behavior in *Drosophila*, has been developed recently²³. In addition to lunging, it would be desirable to measure other aggressive behaviors, such as chasing, tussling, boxing (fencing) and wing threat¹³, as well as courtship behaviors. This would allow the study of whether a given mutation or environmental influence exerts a selective effect on aggression or on social interactions in general²⁴.

Here we describe a machine vision system designed to quantify and analyze various social behaviors in *Drosophila*. Actions associated with courtship, aggression and locomotion are detected from overhead videos of fly pairs. We designed our system, first, to allow detailed, accurate and reproducible quantitative measurements of individual component behaviors ('actions') that are expressed in courtship and/or aggression ('activities'), and second, to enable large-scale genetic and circuit-perturbation screens. The system is simple and inexpensive to build and replicate, functions automatically and permits measurements of multiple fly pairs simultaneously. The application of this approach, together with appropriate multiplex aggression arena configurations²⁵ (**Supplementary Methods** online), should enable large-scale genetic and circuit-based screens of these behaviors.

RESULTS

Hardware and software

We used a double-arena adapted from a recently developed system²³ (**Fig. 1a**). A consumer camcorder, connected to a personal computer, filmed one pair of flies per arena. This setup can be adapted to a medium-throughput mode, consisting of four double arenas (**Fig. 1b–d** and **Supplementary Methods**).

¹Division of Engineering and Applied Science, ²Division of Biology, Howard Hughes Medical Institute, California Institute of Technology, Pasadena, California, USA. Correspondence should be addressed to D.J.A. (wuwei@caltech.edu) or P.P. (perona@caltech.edu).

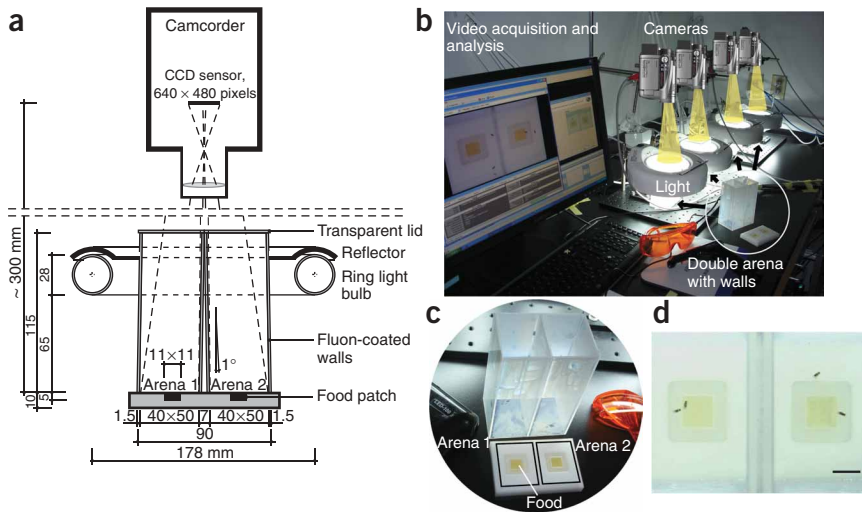


Figure 1 | Imaging setup for genetic screens in *Drosophila*. **(a)** Schematic of a lateral cut through our double chamber (all lengths in mm). CCD, charge-coupled device. **(b)** Example of a medium-throughput behavioral screening assay setup: 4 double chambers, 4 cameras, 2 personal computers and standard video-acquisition software. **(c)** Double chamber with the walls removed to expose the floor. **(d)** Camera view of the double chamber. Each of the two arenas has food in the center, surrounded by agarose; walls are coated with Fluon (Dupont fluoroproducts). Inner walls were tilted by 1° . Scale bar, 10 mm.

Our software (**Supplementary Software** online) consists of six modules: video import, ground truthing, calibration, fly detection and tracking, action detection and graphical user interface. We describe fly detection and tracking as well as action detection here and in **Figure 2**; for other modules, see **Supplementary Methods**.

Detection and tracking

The first step in tracking the flies is computing their silhouette (body and wings) (**Fig. 2a–c**). An important feature of our software is the ability to detect and measure the position of the fly's head and

wings (**Fig. 2c,d**). We illustrate computing the orientation, θ , of a fly in **Figure 2e**. The bodies of abutting flies are resolved by fitting a two-component Gaussian mixture model²⁶ simultaneously to pixel location and brightness (**Fig. 2f** and **Supplementary Methods**).

At each video frame, 25 measurements (features) are computed, characterizing body size, wing pose, and position and velocity of the fly pair (**Fig. 2d,e,g** and **Supplementary Table 1** online). These measurements are the features used to detect actions.

In male–female assays the flies' identity is directly measurable as the female is larger. In male–male assays we painted a white dot on the back of one fly for identification. For unlabeled male–male pairs our software computes the most likely fly-specific trajectories (**Supplementary Methods**).

Action detection

The 25 measured features are used to detect fly actions. Lunging, tussling and wing threat are actions specific to aggression; wing extension (courtship 'song'), circling and copulation are specific to courtship; locomotion and chasing are common to both (**Fig. 3**).

A lunge is defined as one fly rearing briefly on its hind legs and snapping down onto the other fly²³ (**Fig. 3a**, **Supplementary Fig. 1a** online and **Supplementary Videos 1,2** online). Lunging is detected automatically by an example-based classifier in a two-step process (**Supplementary Methods**). First, probable lunges are selected among all frames by using ranges (intervals) on feature

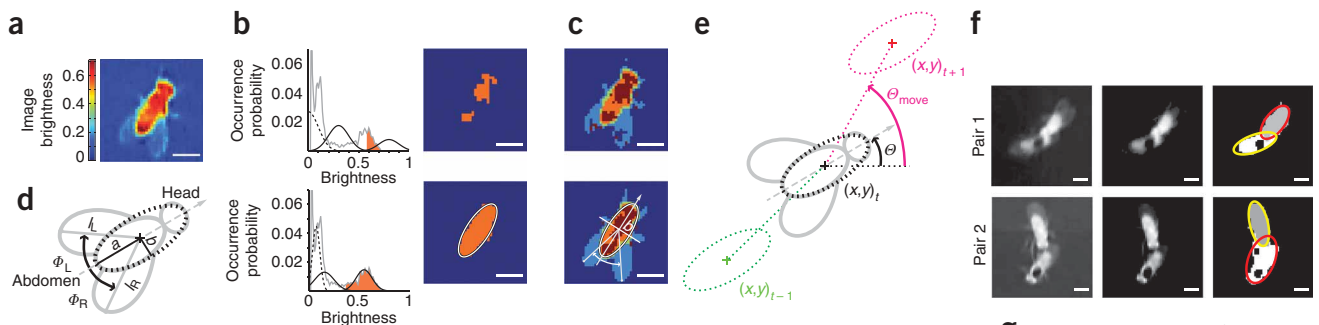


Figure 2 | Detection and tracking of fruit flies. **(a)** 'Foreground image', F_I , computed by dividing the original image I by $\mu_I + 3\sigma_I$ (where μ is the mean and σ is the s.d.; F_I values in false colors). **(b)** The fly body is localized by fitting a Gaussian mixture model²⁶ (GMM) with three Gaussians (background (dashed), other parts and body (solid black)) to the histogram of F_I values (gray) using the expectation maximization (EM) algorithm²⁶. First (top right) and final (bottom right) iterations of the GMM-EM optimization are shown. All pixels with brightness values greater than the value at the intersection of the solid black Gaussians (orange) are assigned to the body and are fit with an ellipse. **(c)** First iteration (top) and final result (bottom) of full fly detection by segmenting the complete fly from the background, with body parts and wings (empirically represented as four segments and colors)³⁰. **(d)** Head and abdomen were resolved by dividing the fly along the minor axis b and comparing the brightness-value distribution of both halves (head is brighter; see **c**). The left and right wings (wing length l_L and l_R ; and wing angle ϕ_L and ϕ_R) were measured by detecting, on each side of the fly's posterior half, the pixel with the furthest distance from the center of the ellipse (wing tip) in the segmented full fly. **(e)** Definition of fly orientation θ and moving direction $\theta_{\text{move}}(t, \text{time})$. **(f)** Separation of occluding (pair 1) and touching flies (pair 2). Original image (left), foreground image (center) and final segmentation result with corresponding ellipses (right) are shown. **(g)** Definitions of additional features. θ_{12} , angle between center of ellipse and head of fly 1 and center of ellipse of fly 2; a , abdomen; h , head; c , center of ellipse; Δ , distance. Scale bars, 1 mm.



Figure 3 | Detectable actions. (a–d) Single images of side and top views showing lunging (a), tussling (b), wing threat (c) and copulation (d). (e,f) Sequential images showing wing extension and circling (e) and chasing (f). Scale bars, 1 mm. Times shown are relative to the first frame in each movie.

values as listed in **Supplementary Table 2** online. Second, probable lunges are accepted or rejected by a k -nearest-neighbor classifier²⁶ using 10 features (**Supplementary Table 3** online). The training examples comprised ~ 250 distinct expert-selected lunge events occurring in 20 min of recorded video for each of 8 fly pairs and a comparable number of negative examples.

We evaluated the performance of our lunge detector on a 20-min movie containing 139 lunges. We obtained ground truth (the accurate identification of all lunges in a movie) in two steps (see Methods and **Supplementary Methods**). We compared the algorithm's performance, as well as a second expert's annotations, to ground truth. The receiver operating characteristic²⁶ representing the fraction of false negatives (lunges present in the ground truth, but not detected) versus the number of false positives (detected, but not present in the ground truth) is shown, as the number of lunge-labeled nearest neighbors that are necessary to declare a lunge is varied (**Fig. 4a**). The threshold we selected for labeling a lunge yielded a detection rate of $\sim 91\%$, representing 126 correct detections, with 13 false negatives and 7 false positives. Lowering the detection threshold decreases the probability for false negatives and increases the number of false positives.

We applied the lunge detector to 56 additional fly-pair movies (**Fig. 4b**) and found excellent agreement with the ground truth, with a correlation of 0.99, a bias of 1.5 lunges and an s.e.m. of 0.40 lunges.

Note that automatic counting is very close to ground truth both when there are many lunges and when there are few.

We could detect other aggressive and courtship actions (see below) by using only the first of the two steps in the example-based classifier algorithm described above. We empirically determined features and ranges for each action by expert analysis of movies containing sample actions. The k -nearest-neighbor classifier step was unnecessary in these cases. We evaluated the performance of our system in detecting the other aggressive and courtship actions using the same approach as in the case of lunging. For all of these behaviors we measured detection rates of 90–100% (**Table 1**).

In aggressive tussling, both flies grip each other with their front legs¹³ (**Fig. 3b**, **Supplementary Fig. 1a** and **Supplementary Video 3** online). The bodies face each other so that their axes of symmetry are parallel (body alignment) and form a single line. Connected solidly in this configuration, they move about in jerks with high velocity and acceleration. To detect and classify aggressive tussling, we compared 8 features to data ranges listed in **Supplementary Table 4** online. When all features are within their empirically determined ranges and this configuration is maintained for 0.3 s or longer, we flagged an aggressive tussling event.

Wing threat is characterized by a lateral extension of both wings by 80 – 90° followed by their elevation to a vertical extension of $\sim 40^\circ$ (**Fig. 3c**, **Supplementary Fig. 1a** and **Supplementary Videos 4,5** online). We observed both rapid, transient elevation of the wings as well as longer-lasting (≥ 0.3 s) occurrences; the latter are typically, but not always, associated with a reduction in walking speed (velocity ≤ 5 mm s^{-1}). In this study, we restricted detection of wing threat to longer-lasting occurrences, as they are more easily discriminated from rapid wing flicking (see **Supplementary Table 5** online for features and ranges).

During courtship, males extend their wings laterally and vibrate them (~ 280 Hz) to produce a courtship 'song' (**Fig. 3e**, **Supplementary Fig. 1b** and **Supplementary Videos 6,7** online). Our system detects wing extension when the angle between the wing and the long axis of the fly body is greater than 60° , the fly is not standing up (fly length, as viewed from the camera, is maximal), and this configuration is maintained for 1 s or longer (see **Supplementary Table 6** online for features and ranges).

Circling is part of courtship and is detected when one fly drifts sideways in a circle with approximately constant velocity around the other fly (**Fig. 3e**, **Supplementary Fig. 1b** and **Supplementary Videos 6,7**; see **Supplementary Table 7** online for features and ranges).

Copulation involves a male fly approaching and mounting a female fly (**Fig. 3d**, **Supplementary Fig. 1b** and **Supplementary Videos 8,9** online). The beginning and end of copulation are characterized by an abrupt change in the distance between the two flies. During copulation their movements become coupled, and locomotion is decreased. Thus, to detect both the starting and ending time-points of copulation, we computed the mean and s.d. of inter-fly distances, Δ_c , within a moving 250-frame (8.3 s) window. We defined the earliest frame when the criteria of mean distance < 2 mm and s.d. < 0.3 mm are simultaneously met as the 'copulation start', and the last such frame as the 'copulation end' (see **Supplementary Table 8** online for features and ranges).

Our system detects chasing when the change of the head-center distance, $\delta\Delta_{h-c}$, between both flies (**Fig. 2g**) is small, both flies have

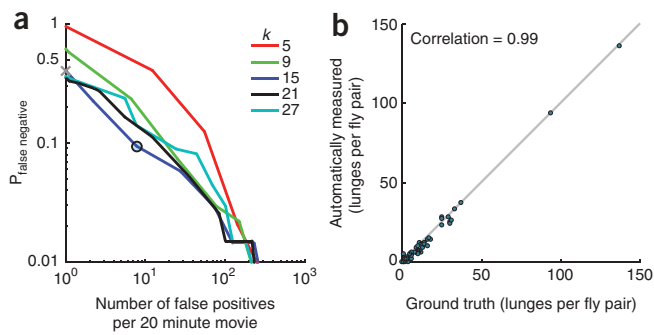


Figure 4 | Performance of action detection. **(a)** Performance of our lunge detector, described by the receiver operating characteristic. Each receiver operating characteristic curve gives the fraction of false-negatives (number of missed lunges divided by the total number of lunges on the ground truth) versus the number of false positives. Curves are shown for different values of k -nearest-neighbors constant k . Best performance was achieved for $k = 15$. The operating point of the system is shown by a black circle; it was obtained by labeling an action 'lunge' when 12 or more of its $k = 15$ nearest-neighbors were lunges. The performance of an expert human observer (40% missed lunges) is indicated by the \times . The expert detected 84 lunges, whereas our two-step process for establishing ground truth yielded 139 lunges. **(b)** Comparison between automatically measured lunges and the number of lunges in the ground truth for each of 56 20-min movies of fly pairs (dots). The gray line is the 45° reference.

the same, constant velocity, the distance between the flies is small but not zero, the chasing fly is oriented toward the chased fly, and the head of the chasing fly is behind the chased fly's abdomen (Fig. 3f, Supplementary Fig. 1c and Supplementary Video 10 online). This configuration has to be maintained for 1 s or longer (see Supplementary Table 9 online for features and ranges).

Genetic and environmental influences on social behavior

To validate the utility of our system for studying experimental perturbations of courtship and aggressive behavior, we first investigated whether it could detect previously described phenotypes produced by gene- or circuit-level manipulations. Octopamine is an insect biogenic amine, which is closely related to mammalian noradrenaline. It is critical in aggressive behavior in *Drosophila*¹⁴. A recent study showed that silencing of octopamine neurons decreases aggressive behavior²³. We performed a similar manipulation, by expressing the inwardly rectifying potassium channel Kir2.1 (ref. 27) in tyrosine decarboxylase 2 (*Tdc2*)-expressing neurons, to suppress their electrical activity. *Tdc2-GAL4; UAS-Kir2.1* flies showed significant decreases in lunging ($P < 0.01$), tussling ($P < 0.05$) and wing-threats ($P < 0.01$) (Fig. 5a–d

and Supplementary Fig. 2a and 3a,b online). There was no significant change in chasing or total distance traveled ($P > 0.05$) (Supplementary Fig. 2b,c).

We also examined flies bearing a mutation in fruitless (*fru*), a sex-specifically spliced transcription factor that specifies gender-dimorphic fly behaviors^{2,4}. Male *fru^F* flies, in which *fru* is spliced into a female-specific (inactive) form, exhibited a strong reduction in male-specific patterns of aggressive behavior (Supplementary Fig. 4a–d online), as previously reported⁴.

We also studied the behavior of *Cha-GAL4; UAS-tra* (Cha-Tra) flies, in which all cholinergic neurons have been feminized owing to misexpression of the transformer gene²⁸. Cha-Tra males exhibited little or no courtship activity toward females, but a robust increase in courtship toward other males (Fig. 5e,f and Supplementary Fig. 2d), at a frequency indistinguishable from wild-type Canton-S male-female pairs.

Cha-Tra male pairs also showed an increase in some aggressive behaviors compared to Canton-S male pairs (Fig. 5g,h, Supplementary Fig. 2e and 3c,d), as previously reported (Y.B. Chan and E.A. Kravitz, *Cold Spring Harbor Laboratory Neurobiology of Drosophila Abstracts*, 42, 2005). In addition, Cha-Tra male pairs had greater locomotor activity (Supplementary Fig. 2f). Lunging activity was significantly higher than in controls ($P < 0.001$), even after normalizing for distance traveled²³ ($P < 0.01$) (Fig. 5i). Wing threat was significantly lower in Cha-Tra flies ($P < 0.01$) (Fig. 5j); thus, not all aggressive actions were more frequent in Cha-Tra flies. Nevertheless, the total time spent in aggressive activity and chasing was significantly elevated in Cha-Tra males ($P < 0.01$ and $P < 0.001$, respectively; Supplementary Fig. 2g,h). Control experiments indicated that copulation could be detected in Canton-S male-female pairs (Supplementary Fig. 2i).

Our software allowed us to compute two-dimensional histograms showing the frequency of actions in each spatial location to detect phenotypes with an altered spatial distribution of behaviors (Supplementary Fig. 5 online). The two-dimensional histograms revealed that Cha-Tra males performed a greater proportion of their tussling bouts on the central food patch, in comparison to controls (Supplementary Fig. 5a). Moreover, the pattern of Cha-Tra fly chasing was more intense around the perimeter of the arena, whereas that in controls was more uniformly distributed (Supplementary Fig. 5b).

We examined ethograms¹³, which illustrate the frequency of each action, as well as the frequency with which one action was followed by the same or another action. We counted intervals > 10 s without action as 'no action' nodes (data not shown). Both Canton-S and Cha-Tra males exhibited multiple transitions between courtship and

Table 1 | Performance evaluation of action detection

Behavior	Number of fly pairs	Number of events	Correct positives (%)	False negatives (%)	Number of false positives	Number of false positives per 20 minute movie	Number of false positives per event
Lunging ^{a,b}	1	139	90.7	9.3	7	7	0.05
Tussling	40	176	Not tested	Not tested	13	0.33	0.07
Wing threat ^{a,c}	40	87	94.3	5.7	4	0.1	0.04
Wing extension ^{d,e}	10	797	96.7	3.3	35	3.5	0.04
Circling ^{d,f}	10	422	99.8	0.2	18	1.8	0.04
Chasing ^g	6	400	98.0	2.0	4	0.67	0.01

^aWild-type Canton-S male-male fly pairs. ^bWe tested 56 additional pairs, and the correlation with ground-truth data was 0.99. ^cWe hand-counted 118 wing threats; 87/118 lasted longer than 0.3 s. False positives were ambiguous situations of wing threat or common wing extension. ^dWild-type Canton-S male-female fly pairs. ^eWe hand-counted 906 single wing extensions; 797/906 lasted longer than 1 s. False positives were due to segmentation errors. ^fOut of 435 hand-counted circling events, 422 had a minimum duration of 1 s. ^g*Cha-GAL4; UAS-tra* male-male fly pairs. Minimum duration, 1 s.

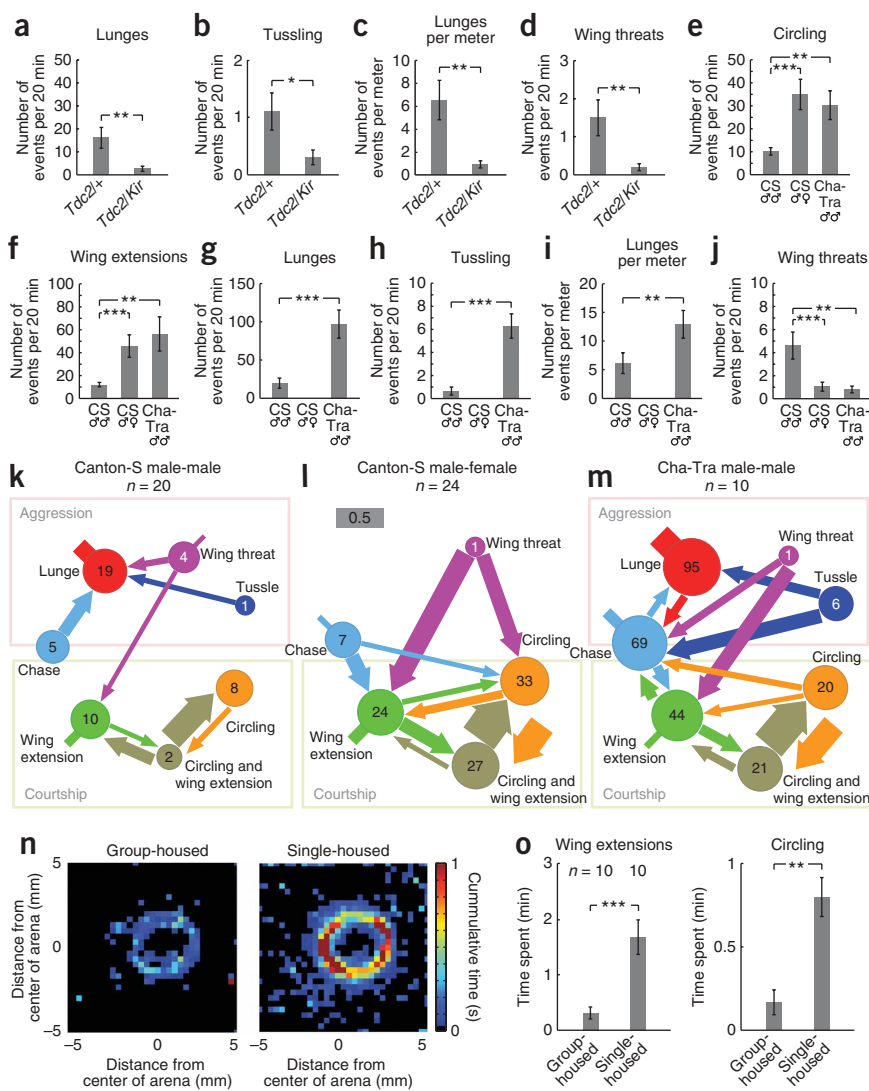


Figure 5 | Genetic and environmental influences on aggressive and courtship behavior. (**a–d**) Number of lunges (**a**), tussling events (**b**), lunges per meter (**c**) and wing threats (**d**) observed in octopamine control (*tdc2^{+/+}*, *n* = 20) and mutant (*tdc2^{+/Kir}*, *n* = 20) flies. (**e–j**) Circling (**e**), wing extensions (**f**), lunges (**g**), tussling (**h**), lunges per meter (**i**) and wing threats (**j**) in Canton-S (CS) male-male (*n* = 20), male-female (*n* = 24) and Cha-Tra (*n* = 10) male-male pairs. Data represent mean ± s.e.m. (**k–m**) Ethograms, based on transition matrices for the indicated flies, showing transitions where the interval between a fly's action and the next action lasted ≤ 10 s. The transition probability is represented by the thickness of the arrows (normalized over all arrows that exit a node including the arrow into 'no action'). The gray bar represents a transition probability of 0.5. The arrow stumps represent the transition probability from one action into the same action. Circle diameters (logarithmically scaled) and numbers denote the average action frequencies. (**n**) Cumulative Canton-S male-fly positions while extending a wing toward a decapitated Canton-S female for group-housed flies (left; *n* = 10) and single-housed flies (right; *n* = 10). (**o**) Time spent performing wing extension and circling by single-housed and group-housed cs male-female pairs. Data represent mean ± s.e.m. **P* < 0.05, ***P* < 0.01 and ****P* < 0.001.

Previous studies have shown that raising post-eclosion *Drosophila* males in social isolation strongly increases aggressiveness, in comparison to flies raised in groups²⁴. We observed that both wing extension and circling were significantly elevated in single-housed versus group-housed flies (*P* < 0.001 and *P* < 0.01, respectively)

(**Fig. 5n,o**). Thus, social isolation increases both male-male aggressiveness and male-female courtship. This poses the question of whether these influences on social behavior are mediated by common or distinct mechanisms.

DISCUSSION

Our software detects wing postures, permitting measurements of wing threat and wing extension. Wing threat, in particular, is an interesting and important aggressive display because it is independent of locomotor activity. Indeed, we found that a genetic manipulation (Cha-Tra) that strongly increases lunging, tussling and chasing, decreased wing threat.

The time saved by our software is enormous. It takes us at least one hour to score manually one type of action in one 20-min fly-pair movie. To characterize aggression and courtship in a line of flies (all 8 actions in, for example, 12 fly pairs), one would require ~100 h of manual labor, as opposed to a few minutes to set up and run our system. As an example, the three ethograms presented in **Figure 5** would have taken ~270 person-hours to prepare. This capability affords the opportunity to compare multiple genotypes or wild-type genetic backgrounds, which would be virtually impossible to do manually.

aggressive activities (**Fig. 5k–m**). Cha-Tra males additionally showed transitions between aggression and courtship and vice versa. They also showed an elevated amount of chasing activity. In Canton-S male pairs, chasing was followed most often by lunging, whereas in Cha-Tra males, chasing was followed with equal probability by either lunging, an aggressive action, or by wing extension, a courtship action (**Fig. 5k,m**). By contrast, in Canton-S male-female pairs, chasing by males was followed most often by wing extension (**Fig. 5l**). One interpretation is that in Canton-S male-male pairs, chasing is primarily an aggressive action, whereas in male-female pairs it is primarily a courtship action. In Cha-Tra male-male pairs, chasing may be indicative of either aggression or courtship, suggesting that these flies may have a deficit in gender recognition or discrimination. This observation is consistent with a recent study²⁹ reporting that feminization of octopaminergic and tyraminerbic neurons by misexpression of Tra caused male-directed wing extensions to be followed primarily by male-male courtship.

Finally, to examine the effects of social experience, an environmental influence, on male-female courtship, we used our software to analyze wing extension and circling, two male-specific courtship actions. In this courtship assay the male was in the presence of an immobilized (decapitated) female in the center of the arena.

The ability to monitor simultaneously both aggressive and courtship activities allows the computation of ethograms. This may prove to be valuable in determining whether aggression and courtship actions are part of a social behavior ‘continuum’ or whether these two activities represent discrete ‘states’ with ‘state transitions’ controlled by different circuits. Genetic or circuit-based screens can be performed to search for phenotypes that affect not only the ability to perform a particular action, but also that affect the probabilities of transition between actions.

Our system is completely automatic and self-calibrating; using it does not require special training, provided that the hardware setup is well reproduced. It has been designed for inexpensive implementation and easy replication. Fly behavior may be measured accurately in smaller arenas, allowing us to simultaneously monitor an array of arenas with each camera, thus permitting large-scale genetic screens with high throughput. Together, these features should open up aggression and courtship to powerful genetic screens. This in turn should help to illuminate the genes and neural circuits that control these important social behaviors and may reveal general principles of the organizational logic or control mechanisms that are evolutionarily conserved.

METHODS

Fly stocks and rearing conditions. Flies were reared in plastic vials containing standard fly medium (yeast, corn syrup and agar) at 25 °C, 60% humidity with a 12 h light-dark cycle. Newly eclosed males were single housed or group housed (10 flies per vial) for 4–6 days before we performed the behavioral assay. Virgin Canton-S females were collected shortly after eclosion and raised at 20 flies per vial for 4–6 d before we performed the courtship assay. *Cha-GAL4;UAS-tra* flies were made by crossing male *UAS-transformer* to female *Cha-GAL4* flies. The *fru^F* mutant was recently generated². *Tdc2-GAL4;UAS-Kir2.1* flies were made by crossing male *Tdc2-GAL4* flies to female *UAS-Kir2.1* flies.

Aggression assay. We introduced two males of the same age into the double-arena setup by gentle aspiration without anesthesia and immediately video-captured them for 20 min. The temperature and humidity of the apparatus were set to ~25 °C and ~40%, respectively.

Courtship assay. Two types of courtship assays were performed. The apparatus and environmental conditions were as used in the aggression assay. One male and a virgin female were introduced into the apparatus by gentle aspiration without anesthesia and immediately video-captured for 30 min (24 pairs) to cover the copulation period. For all other actions only the first 20 min were analyzed. In another assay the female was decapitated and placed in the center of the food patch and replaced every hour. After the male was introduced into the apparatus both flies were immediately video-captured for 10 min.

Training and ground-truth data. We collected a hand-annotated database of lunging, wing threat, chasing, wing extension and circling to train our software and to measure its performance. Data used to train the detectors were produced by a human observer without additional checks. Data that were used for testing the system’s performance were further processed to obtain a reliable ‘ground truth’. Human experts tend to miss relevant events (in our observations, 30–40% of events are missed) for two reasons.

(i) Different human observers use slightly different criteria, even when they agree on the overall action definition. (ii) A human observer’s attention level changes over time during movie annotations. Therefore, to obtain reliable ground truth for performance testing, we devised an improved two-step procedure involving two experts (**Supplementary Methods**).

Statistical analyses. Kruskal-Wallis ANOVA was applied to detect overall differences among the unpaired groups. Significantly different groups were compared pairwise by the Mann-Whitney U-test. For all multiple comparisons, Bonferroni correction was applied.

Graphical user interfaces and software availability. Our software (**Supplementary Fig. 6a,b** and **Supplementary Software** online; software available as an executable file.) was run from graphical user interfaces allowing the user to visualize tracking and statistical data. Software source code is available free to academic and nonprofit investigators upon request. Commercial entities should contact the Caltech Office of Technology Transfer for licensing arrangements. Software updates will be available at <http://vision.caltech.edu/cadabra/>.

Additional methods. Additional information on the software, detection and tracking as well as method hardware is available in **Supplementary Methods**.

Note: Supplementary information is available on the Nature Methods website.

ACKNOWLEDGMENTS

We thank K. Watanabe and A. Hergarden for helping prepare the flies, assays, taking video footage of flies as well as collecting ground-truth data. This work was supported by a National Science Foundation Frontiers in Integrative Biological Research grant to M.J. Dickinson, D.J.A. and E. Isacoff, a National Science Foundation National Institutes of Health grant to P.P. and M.J. Dickinson, and a postdoctoral fellowship of the Alexander von Humboldt-Foundation to H.D. We thank M. Heisenberg for sponsoring H.D. in Germany and for sharing information and data regarding aggression arenas and automated assays.

Published online at <http://www.nature.com/naturemethods/>
Reprints and permissions information is available online at <http://npg.nature.com/reprintsandpermissions/>

- Manoli, D.S. *et al.* Male-specific fruitless specifies the neural substrates of *Drosophila* courtship behaviour. *Nature* **436**, 395–400 (2005).
- Demir, E. & Dickson, B.J. fruitless splicing specifies male courtship behavior in *Drosophila*. *Cell* **121**, 785–794 (2005).
- Stockinger, P., Kvitsiani, D., Rotkopf, S., Tirian, L. & Dickson, B.J. Neural circuitry that governs *Drosophila* male courtship behavior. *Cell* **121**, 795–807 (2005).
- Vrontou, E., Nilsen, S.P., Demir, E., Kravitz, E.A. & Dickson, B.J. fruitless regulates aggression and dominance in *Drosophila*. *Nat. Neurosci.* **9**, 1469–1471 (2006).
- Manoli, D.S., Meissner, G.W. & Baker, B.S. Blueprints for behavior: genetic specification of neural circuitry for innate behaviors. *Trends Neurosci.* **29**, 444–451 (2006).
- Callaway, E.M. A molecular and genetic arsenal for systems neuroscience. *Trends Neurosci.* **28**, 196–201 (2005).
- Luo, L., Callaway, E.M. & Svoboda, K. Genetic dissection of neural circuits. *Neuron* **57**, 634–660 (2008).
- Suh, G.S. *et al.* A single population of olfactory sensory neurons mediates an innate avoidance behaviour in *Drosophila*. *Nature* **431**, 854–859 (2004).
- Katsov, A.Y. & Clandinin, T.R. Motion processing streams in *Drosophila* are behaviorally specialized. *Neuron* **59**, 322–335 (2008).
- de Bono, M. & Maricq, A.V. Neuronal substrates of complex behaviors in *C. elegans*. *Annu. Rev. Neurosci.* **28**, 451–501 (2005).
- Skrzipek, K.H., Kroner, B. & Hager, H. Inter-male aggression in *Drosophila melanogaster*—laboratory study. *J. Comp. Ethol.* **49**, 87–103 (1979).

12. Hoffmann, A.A. A laboratory study of male territoriality in the sibling species *Drosophila melanogaster* and *D. simulans*. *Anim. Behav.* **35**, 807–818 (1987).
13. Chen, S., Lee, A.Y., Bowens, N.M., Huber, R. & Kravitz, E.A. Fighting fruit flies: a model system for the study of aggression. *Proc. Natl. Acad. Sci. USA* **99**, 5664–5668 (2002).
14. Kravitz, E.A. & Huber, R. Aggression in invertebrates. *Curr. Opin. Neurobiol.* **13**, 736–743 (2003).
15. Greenspan, R.J. & Ferveur, J.F. Courtship in *Drosophila*. *Annu. Rev. Genet.* **34**, 205–232 (2000).
16. Wehrhahn, C., Poggio, T. & Bülthoff, H. Tracking and chasing in houseflies (*Musca*). *Biol. Cybern.* **45**, 123–130 (1982).
17. Branson, K. & Belongie, S. Tracking multiple mouse contours (without too many samples). *IEEE Computer Vision and Pattern Recognition* **1**, 1039–1046 (2005).
18. Khan, Z., Balch, T. & Dellaert, F. MCMC-based particle filtering for tracking a variable number of interacting targets. *IEEE Trans. Pattern Anal. Mach. Intell.* **27**, 1805–1819 (2005).
19. Veeraraghavan, A., Chellappa, R. & Srinivasan, M. Shape-and-behavior encoded tracking of bee dances. *IEEE Trans. Pattern Anal. Mach. Intell.* **30**, 463–476 (2008).
20. Fry, S.N., Rohrseitz, N., Straw, A.D. & Dickinson, M.H. TrackFly: virtual reality for a behavioral system analysis in free-flying fruit flies. *J. Neurosci. Methods* **171**, 110–117 (2008).
21. Wolf, F.W., Rodan, A.R., Tsai, L.T. & Heberlein, U. High-resolution analysis of ethanol-induced locomotor stimulation in *Drosophila*. *J. Neurosci.* **22**, 11035–11044 (2002).
22. Valente, D., Golani, I. & Mitra, P.P. Analysis of the trajectory of *Drosophila melanogaster* in a circular open field arena. *PLoS ONE* **2**, e1083 10.1371/journal.pone.0001083 (2007).
23. Hoyer, S.C. *et al.* Octopamine in male aggression of *Drosophila*. *Curr. Biol.* **18**, 159–167 (2008).
24. Wang, L., Dankert, H., Perona, P. & Anderson, D.J. A common genetic target for environmental and heritable influences on aggressiveness in *Drosophila*. *Proc. Natl. Acad. Sci. USA* **105**, 5657–5663 (2008).
25. Dierick, H.A. A method for quantifying aggression in male *Drosophila melanogaster*. *Nat. Protoc.* **2**, 2712–2718 (2007).
26. Bishop, C.M. *Pattern Recognition and Machine Learning* (Springer, New York) p. 738 (2007).
27. Johns, D.C., Marx, R., Mains, R.E., O'Rourke, B. & Marban, E. Inducible genetic suppression of neuronal excitability. *J. Neurosci.* **19**, 1691–1697 (1999).
28. Ferveur, J.F., Stortkuhl, K.F., Stocker, R.F. & Greenspan, R.J. Genetic feminization of brain structures and changed sexual orientation in male *Drosophila*. *Science* **267**, 902–905 (1995).
29. Certel, S.J., Savella, M.G., Schlegel, D.C.F. & Kravitz, E.A. Modulation of *Drosophila* male behavioral choice. *Proc. Natl. Acad. Sci. USA* **104**, 4706–4711 (2007).
30. Otsu, N. A threshold selection method from gray level histograms. *IEEE Trans. Syst. Man Cybern.* **9**, 62–66 (1979).